

Stereolithography of ceramic suspensions

A. GRECO

*Dipartimento ingegneria dell'innovazione, Università di Lecce,
via per Arnesano 73100 Lecce, Italy*

A. LICCIULLI

PASTIS-CNRSM, SS 7 Km 7+300, 72100 Brindisi, Italy

A. MAFFEZZOLI*

*Dipartimento ingegneria dell'innovazione, Università di Lecce,
via per Arnesano 73100 Lecce, Italy*

E-mail: alfonso.maffezzoli@unile.it; maffez@axpmat.unile.it

The need of fast production of prototypes of complex shapes in very short time lead to the development in the last years of many additive rapid prototyping (RP) technologies for the production of single objects or of very limited series. The new fabrication concept allowed the construction of complex parts, starting from a 3D-CAD model, without using a mould. However, most of these additive processes produce polymeric objects and only recently the laser sintering of metal powders has been commercially introduced. In this work the production of ceramic objects by stereolithography is presented starting from the development of UV curable pre-ceramic suspensions for free form fabrication of alumino-silicate parts. The suspensions are characterized by 40%–50% by volume of powder content and by a reactivity and a viscosity compatible with their application in stereolithography. The ceramic green is built in a stereolithographic system operating with a He-Cd laser (325 nm). Then, the ceramic objects are obtained by pyrolysis of the organic binder and subsequent sintering of the green at 1600 °C. Finally, a characterisation of the mechanical properties and of the microstructure of the samples is presented.

© 2001 Kluwer Academic Publishers

1. Introduction

The need of fast production of prototypes of complex shape in very short time lead to the development from the mid 80's of many additive rapid prototyping (RP) technologies for the production of single objects or of very limited series [1]. The new fabrication concept allowed the construction of complex parts, starting from a 3D-CAD model, without using a mould. In RP, the object building is obtained bonding, layer by layer, its sections by an additive process rather than cutting or «sculpturing» the parts from an homogeneous block. The key point of RP is given by the direct link between the CAD model and the solid object, generated in few hours suggesting that tailor made or single functional parts could be fabricated for example for prosthetic applications in very a short time. However, most of the RP processes produce polymeric objects and only recently the laser sintering of metal powders [2] has been commercially introduced. The poor thermal and mechanical properties of the polymeric materials used for rapid prototyping makes attractive the generation of metallic or ceramic prototypes for functional testing.

In the last years, the significant efforts devoted to the development of technologies of RP based on non-

polymeric materials lead to the market equipments based on the selective laser sintering of metallic powders. On the other hand, the use of ceramic materials in RP is applied at laboratory level in different processes:

- LOM (Laminated Object Manufacturing). Object building is commonly performed by sequentially cutting, stacking and bonding sheets of paper. Therefore, LOM technology can be exploited for building ceramic or ceramic matrix composites parts using sheets of ceramics or fiber reinforced ceramic prepregs [3].
- FDM (Fused Deposition Modelling). Usually a thermoplastic polymer is extruded and the object is built layer by layer according with the CAD data. The application to RP ceramic processing is obtained extruding a suspension of a ceramic powder and a thermoplastic binder [4]. The green parts must be heated in order to burn the binder and to sinter the ceramic [2].
- DCJP (Direct Ceramic Jet Printing). In this process a ceramic powder is dispersed in a liquid medium suitable for a modified ink jet system that is used for building the parts layer by layer. Multilayer objects

* Author to whom all correspondence should be addressed.

can be obtained loading different ink jet heads with more than one type of ceramic powder [4].

- SLS (Selective Laser Sintering). Thin layers of ceramic, metallic or polymeric powders are selectively sintered using a laser beam (typically CO₂) of high power [5]. The laser beam moves on the surface of a vat filled with powder according with the desired section geometry and the objects are still built adding further layers. One advantage of this process is related with the direct production of ceramic parts, skipping the production of the intermediate green. The direct sintering of ceramic powders is still at development stage as a consequence of the costs associated with the high power and temperatures required for sintering of ceramic.
- STL (Laser Stereolithography) [1]. This represents the most assessed process for rapid prototyping and can be adapted to building of ceramic objects. The objects are obtained polymerising a low viscosity liquid resin layer by layer. The shape and the dimensions of the parts are directly transferred from a three dimensional CAD system to the stereolithography equipment where a laser beam (usually He-Cd or Ar) polymerises the different sections. Suspensions of ceramic powders in a photoreactive resin can be used in a standard STL equipment in order to build green parts [6].

In this work the production of ceramic objects using a stereolithographic apparatus is presented. UV curable pre-ceramic suspensions for alumino-silicate parts have been studied using photocalorimetric and rheologic characterisations. Thermogravimetry and dilatometry have been used in order to analyse the behaviour of the preceramic green during thermal treatment. An experimental set-up made of an He-Cd laser moving along two horizontal axis and a platform moving in the vertical direction has been used to build layer by layer green bars. The ceramic objects have been obtained by pyrolysis of the organic binder and subsequent sintering of the green at high temperature. Finally, a characterisation of the mechanical properties and of the microstructure of the samples has been performed.

2. Experimental

2.1. Materials

The adopted suspensions are prepared on the base of proprietary resin formulations obtained using commercially available acrylic and silicon acrylate monomers (Table I). The silica yield resulting from pyrolysis of silicone acrylate resins is also reported Table I. The resin is loaded with alumina powder AES 23 (alumina

easy sintering) from Sumitomo, possessing a density after sintering of 3.77 g/cm³ (fired density at 1600 °C), a mean particle size of 1.8 μm, a surface area of 0.42 m²/g and a linear shrinkage on sintering of about 16%. The filler volume fraction used for the three studied suspensions is reported in Table I. In every formulation 3 phr of 1-hydroxy-cyclohexyl-phenyl-ketone Irgacure 184 from Ciba, as photoinitiator, is added.

2.2. Characterisation techniques

Every formulation needs to be evaluated in terms of reactivity, viscosity, behaviour during thermal treatment, and finally mechanical properties of ceramic parts have to be tested. The techniques involved in materials characterisation are the following:

- Differential Scanning Calorimetry (DSC). The cure of the resin was carried out in air at 25 °C in a DSC Perkin Elmer DSC-7. The DSC is modified for irradiation of the sample using transparent quartz windows. The light reaching the sample, produced by a 300 W Xenon lamp Cermax LX 300, is limited to a wavelength interval of 325 ± 4 nm using a monochromator, in order to simulate the irradiation band of a He-Cd laser beam. The beam is focused on the sample using a system of lenses and a mirror. The light intensity is modulated using a series of neutral filters and is measured at the beginning of each experiment using a power meter OPHIR PD2A. The heat generated by the light is negligible at the used UV wavelength.
- Rheology. The viscosity of suspensions at 25 °C as a function of the amount of filler loaded is measured using a stress controlled rheometer Bohlin CS.
- Thermogravimetry (TGA) and thermomechanical Analysis (TMA). The behaviour of the preceramic green samples during pyrolysis of the organic binder and sintering is studied using TGA, Netzsch STA 406. Dimensional changes associated with pyrolysis and sintering are measured by a TMA, Netzsch TMA 402.
- Mechanical testing. Three point bending test of sintered ceramic specimens are performed using a dynamometer Instron 4507.

2.3. Stereolithography apparatus

The STL apparatus is composed of the following parts assembled according to the sketch of Fig. 1:

- A laser He-Cd, from Omnicrome series 3056, with a specific power of 17 mW/mm², emitting at the wavelength of 325 nm, and with a beam diameter of 0.2 mm;
- A scan system, which drives the laser beam on the suspension surface;
- A software which controls the scan system allowing the construction of rectangular parts scanning the vat surface along parallel lines. The parameters which can be controlled are the scanning direction, the dimension of the part, the scan speed and number of scans per unit width. The energy per unit

TABLE I Composition of the studied formulations

| Formulation | Alumina content (vol. %) | Silicone acrylate resin (vol. %) | Other acrylate resin (vol. %) | Silica yield of silicone acrylate (weight %) |
|-------------|--------------------------|----------------------------------|-------------------------------|--|
| XMA | 55 | 50 | 50 | 30 |
| TMA2 | 45 | 100 | 0 | 24 |
| THA2 | 50 | 30 | 70 | 21 |

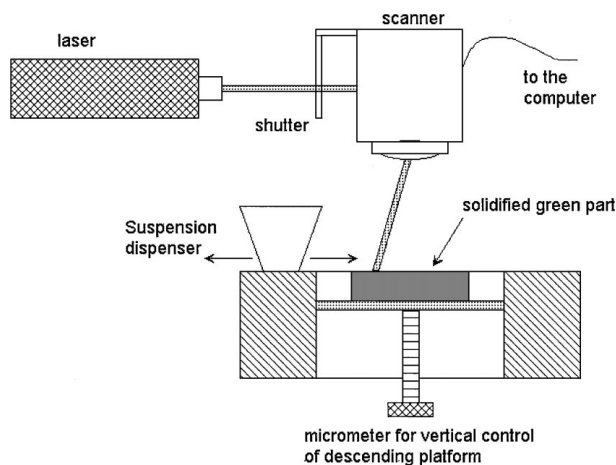


Figure 1 Sketch of the experimental stereolithographic apparatus.

area was controlled by properly setting the last two parameters;

- A moving platform with manual control, which can move downward to build a new layer after suspension re-filling.

3. Results and discussion

3.1. Formulation of suspensions

Different formulations of base resin for ceramic suspension have been prepared with the aim of maximising the reactivity and minimising the viscosity. The use of a silicone acrylate resin is considered a key factor in order to obtain a solid residue of silica after pyrolysis of the organic binder in the suspensions. This residual silica could reduce the shrinkage and improve the sintering by reacting with alumina particles.

The modified differential scanning calorimeter described above is used for the comparison of the rate of reaction of the formulations with commercial resins. In particular two commercial resins from Ciba were selected: a very reactive acrylic based resin, XB5149 and an epoxy based resin SL5170 characterised by lower reactivity. The kinetic properties of XB5149 are considered as an upper limit of reactivity and those of SL5170 as a lower limit of reactivity for effective use in STL.

A typical DSC thermogram obtained on the resin XB5149 at a constant temperature of 25 °C is reported in Fig. 2. When the shutter is opened and the sample

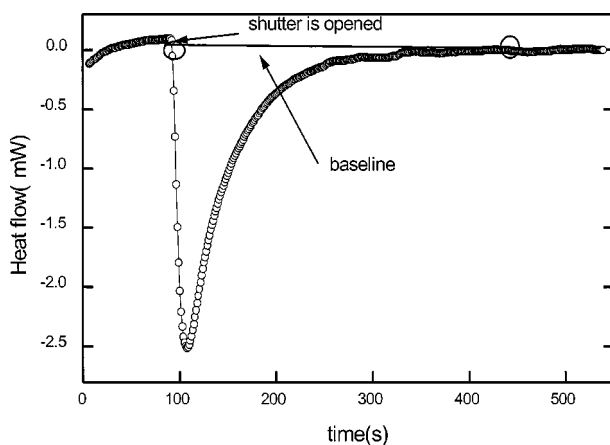


Figure 2 DSC analysis of the commercial resin XB5149.

is exposed an exothermal heat flow is immediately detected. The measured signal goes through a maximum and then returns to the baseline value during continuous irradiation of the sample. The DSC measurements are commonly used for determination of the advancement of the polymerisation by assuming that the heat evolved during polymerisation reaction is proportional to the overall extent of reaction given by the fraction of reactive groups consumed. Following this approach the degree of reaction, α , is defined as:

$$\alpha = \frac{Q(t)}{Q_{\text{tot}}} \quad (1)$$

where $Q(t)$ is the partial heat of reaction developed during a DSC experiment and Q_{tot} represents the total heat of reaction measured when the reaction is completed. The reaction rate, $d\alpha/dt$, is thus obtained from the heat flow dQ/dt as:

$$\frac{d\alpha}{dt} = \frac{1}{Q_{\text{tot}}} \left(\frac{dQ}{dt} \right) \quad (2)$$

The time dependence of the degree of reaction calculated by DSC for the neat resins used for the suspensions of Table I is compared in Fig. 3 with the behaviour of the STL resins SL 5170 and XB 5149. As shown in this figure, the time to reach full conversion for the resin used for the XMA and TMA2 suspensions are lower than that of SL5170 indicating that adequate reactivity for the use in commercial equipment is obtained for the neat resin.

Furthermore, it can be noted that the time to reach full conversion for neat resin used in XMA formulation is much greater than the time needed for the conversion of XB5149; this is a consequence of the presence in this formulation of a monofunctional silicone-methacrylate. However, the presence of a monofunctional methacrylate is chosen since it is responsible of a significant decrease in the viscosity.

The resins, formulated with the aid of DSC experiments, have been filled with different amount of alumina according with the data reported in Table I. These suspensions have been further characterised on the basis of their working parameters with the STL apparatus.

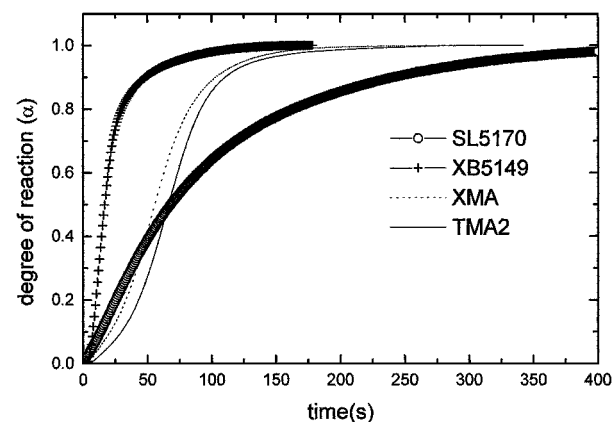


Figure 3 Plot of the degree of reaction vs. time of different commercial resins and formulations for green pre-ceramic.

The reactivity of a STL resin is characterised by two parameters relating the cure depth with the energy dose at the vat surface (E_o) [1]:

$$C_d = D_p \ln \frac{E_o}{E_c} \quad (3)$$

where the working parameters D_p and E_c , are the penetration depth and critical energy respectively and the cure depth (C_d) represents the thickness of gelled resin. E_c is the minimum value of energy needed to polymerise the resin in the suspension, while D_p is a characteristic parameter proportional to the gelled thickness. In order to obtain an adequate depth of cure with a low energy dose E_o , a resin should have high values of D_p and low values of E_c .

The working parameters of suspensions are calculated measuring the hardened thickness at different values of E_o . A linear regression on experimental C_d values plotted as a function of $\ln E_o$ (Fig. 4), is used for the determination of D_p and E_c from the slope and the intercept respectively. These working curves are compared in Fig. 4 with those obtained for commercial resins XB5149 and SL5170 using literature values of D_p and E_c [7]. The calculated and reference values are listed in Table II.

From the results reported in Fig. 4 and Table II, it can be observed that for all the suspension the slope is higher (lower D_p) than for neat commercial resin. However, the suspensions XMA and THA2 present a very low energy E_c , even lower than that of XB5149. In terms of penetration depth, the better performances

TABLE II Working parameters of adopted formulations and commercial resins

| Formulation | E_c (mJ/cm ²) | D_p (mm) |
|-------------|-----------------------------|------------|
| XMA | 1.2 | 0.034 |
| TMA2 | 56 | 0.085 |
| THA2 | 6.4 | 0.073 |
| TH | 8.6 | 0.24 |
| XB5149* | 5.5 | 0.18 |
| SL5170* | 13.5 | 0.12 |

*Values from the resin supplier [7].

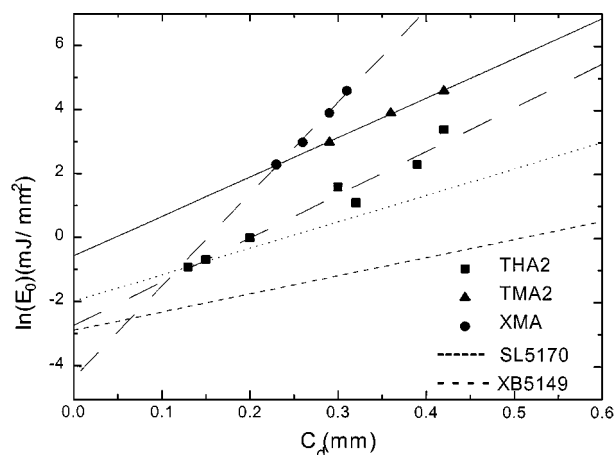


Figure 4 Working curves for suspensions in Table I compared with working curves of commercial STL resins.

are displayed by the THA2, though not being the less filled suspension. The hardening of THA2 requires similar energy of SL5170 for a layer thickness between 0.1 and 0.2 mm. This result is interesting considering that THA2 is loaded with about 50% by volume of alumina, which should decrease the reactivity of the suspension by light scattering. This is more evident in Table II, where the values of the working parameters for the base resin for suspension THA2, called TH, are reported. It can be noted the negative influence of the presence of alumina on the reactive properties of the resin, especially concerning the penetration depth. Although a lower content of filler is used in TMA2, the presence of a monofunctional methacrylate component leads to low reactivity resulting in a high E_c . It can be concluded that the effect of the filler on D_p is very significant while the critical energy, measuring the reactivity at the surface of the suspension, is essentially dependent on the resin formulation independently from the amount of filler.

In Fig. 5 a comparison of the viscosity of two different suspensions, prepared with the same resin, but containing 50% and 55% by volume of alumina, is reported. The alumina is also responsible of a strong increase of the viscosity of the suspensions. The phenomenon becomes critical especially when the powder content exceeds 50% in volume. The increase in viscosity at low shear stress, those of interest for stereolithography, is about four orders of magnitude by simply adding 5% of alumina, while the difference is less evident at higher values of shear stress.

TGA and TMA analysis have been used to identify the temperature intervals interested by pyrolysis and sintering. The weight loss of the base resin for suspension XMA is shown in Fig. 6. The resin burn out occurs up to 700 °C with a weight loss of about 85%. Two degradation steps are detected in Fig. 6: the first can be attributed to the degradation of acrylates and the second to silicone acrylate monomers. At higher temperatures the weight of the sample stabilises and no other phenomena can be monitored during the TGA analysis. Upon heating to these high temperatures, a solid residual can be observed corresponding to the formation of a silica phase from pyrolysis of silicone acrylate resin.

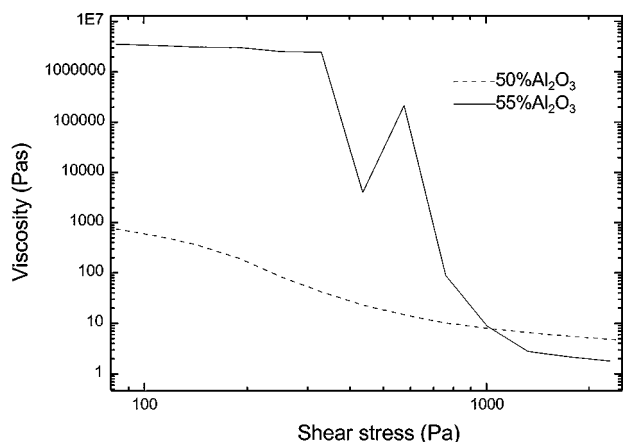


Figure 5 Comparisons of two different suspensions with the same base resin but containing 50 and 55% volume of alumina.

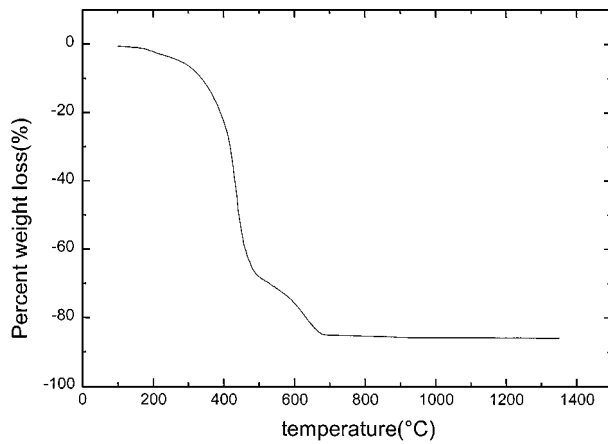


Figure 6 Thermogravimetric analysis of the base resin used for XMA suspension.

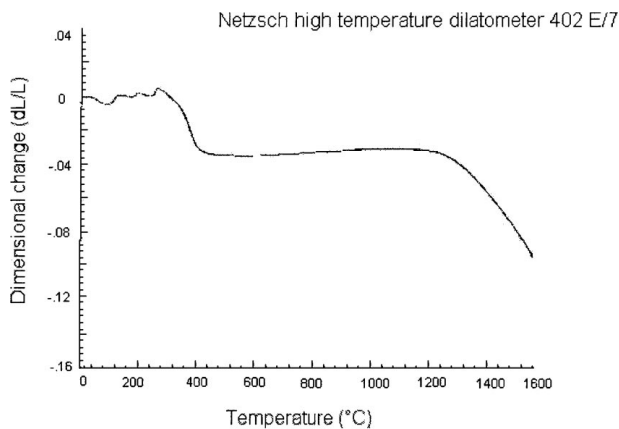


Figure 7 TMA analysis of a ceramic part built from XMA suspension.

The dilatometric analysis of a green sample made with the suspension XMA is reported in Fig. 7. The resin burn-out at temperatures up to 500°C leads to a shrinkage of the ceramic part and to the formation of a porous body characterised by 55 m²/g of surface area. The silica derived from silicone acrylate pyrolysis, characterised by micro and meso porosity, can be responsible of the observed surface area. Then between 500°C and 1100°C a plateau is observed followed by a second significant dimensional change. In this temperature range, the mass of the specimen does not change indicating that the ceramic powder undergoes sintering with an increase in density and decrease of the surface area to zero.

The changes of these parameters during heating of the suspension XMA are reported in Table III: the burn-out of resins with an associated shrinkage (Figs 6 and 7), which occurs between 100°C and 500°C, leads to an increase of density and of surface area. Then, during sintering of the ceramic powders, the density increases because of the reduction of internal voids and the decrease of surface area. The use of a silicone resin is

TABLE III Variation of density and surface area as a function of temperature during thermal treatment of XMA suspension

| Temperature (°C) | 100°C | 550°C | 1550°C |
|----------------------------------|-------|-------|--------|
| Density(g/cm ³) | 2.847 | 3.53 | 3.72 |
| Surface area (m ² /g) | 0 | 55 | 0 |

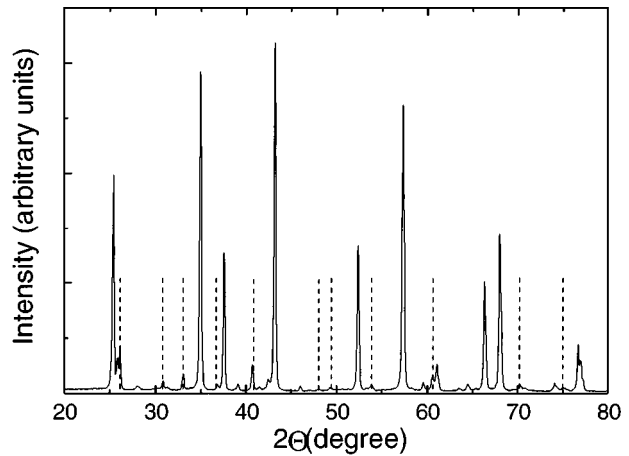


Figure 8 X-ray diffraction analysis for ceramic sintered part built from XMA. Dashed lines indicate mullite phase, other peaks are attributed to alumina.

responsible of a solid silica residue that limits excessive shrinkage and improves sintering of alumina particles.

X-ray diffraction analysis, reported in Fig. 8, shows the sharp and intense peaks of Al₂O₃ phase while the less intense and broader peaks are attributed to small crystallites of mullite produced by the reaction between silica and alumina at particle boundaries.

Following the indications of TGA and TMA experiments the resin burn out between 200°C and 500°C must be very slow, because in this phase the intense shrinkage can determine thermal stresses. The overall thermal treatment has then been divided into three steps:

- Post-cure: the green ceramic part is held in a furnace at 160°C for 100 min, in order to allow a complete reaction of the resin eventually not fully reacted at the end of the laser exposure. The resulting pre-ceramic green is characterized by poor mechanical properties because of the presence of the resin which is also responsible of low density values;
- pyrolysis: heating at about 60°C/h to 500°C. This is a very delicate phase where the resin burn-out is accompanied by an increase of density and a resulting shrinkage;
- sintering: heating from 500°C to 1550°C at 300°C/h. The fraction of voids in the ceramic is reduced with a significant increase of density.

3.2. Ceramic parts manufacturing

The ceramic parts have been obtained by laser exposure of each layer to an energy dose of 10 mJ/mm². The thickness of each layer has been chosen to be 0.1 mm, resulting a good compromise between cure depth, processing times and shape tolerances. In order to obtain a ceramic piece about 3 cm thick 30 layers are needed.

The dimensions of the pre-ceramic parts, as they were produced directly in the SLA, and of the ceramic, obtained after complete thermal treatment, are reported in Table IV. It must be noted that the dimensions of cured parts is higher than those imposed by the software driving the laser. In a typical STL process the resulting

TABLE IV Dimensions of green pre-ceramic specimen and of fully sintered ceramic parts obtained using a 45×5 mm scan area and 32 layers of 0.1 mm of thickness for THA2 and 33 layers of 0.1 mm for TMA2. XMA parts are obtained using a 40×10 mm scan area and 27 layers of 0.1 mm of thickness

| Formulation | Length (mm) | Width (mm) | Thickness (mm) |
|---------------|-----------------|-------------------|------------------|
| TMA2 | 46.8 ± 0.05 | 5.36 ± 0.001 | 3.32 ± 0.001 |
| TMA2 sintered | 43.0 ± 0.1 | 4.23 ± 0.01 | 2.37 ± 0.01 |
| THA2 | 47.9 ± 0.05 | 5.61 ± 0.001 | 3.43 ± 0.001 |
| THA2 sintered | 41.5 ± 0.1 | 4.87 ± 0.01 | 3.13 ± 0.01 |
| XMA | 42.5 ± 0.05 | 10.22 ± 0.001 | 2.87 ± 0.001 |

solidified line under laser beam exposure has a finite linewidth. This width is dependent upon beam diameter and resin working parameters. Therefore the resulting part is oversized by one half the cured linewidth on all borders. In STL software linewidth compensation is entered as dimension representing half the cured linewidth [1]. However in this case the linewidth is of only 0.2 mm, leading to a size increase of 0.2 mm at the borders of the scanned area. The larger dimension measured (Table IV) can result from light scattering produced by the alumina particles at the boundaries of the exposed area. The comparison of the two tables indicates that the overall shrinkage after pyrolysis and sintering is about 8% and 21% for TMA2 in the direction of length and width, respectively, while for THA2 the relative values are both 13%. The measured values of density for the ceramic parts obtained from XMA and THA2 are compared in Table V. The higher value of density obtained for XMA is essentially due to the higher alumina content in the suspension. The improved reactivity of THA2 suspension, obtained increasing the amount of multifunctional-acrylate monomers not containing silicon atoms and reducing the alumina content, is counteracted by a lower sintered density. It must be noted that the theoretic densities reported in Table II have been obtained using an alumina density of 3.77 g/cm^3 . This value corresponds to the limit, after sintering, of the used powder. If the density of bulk alumina would be assumed to be 3.96 g/cm^3 , the calculated density for the silica/alumina ceramic would result higher than 3.77 g/cm^3 , while this value represents the maximum density that could be achieved sintering the neat alumina powder.

3.3. Mechanical properties

The results of three point bending tests, performed on the ceramic parts obtained from the three formulations, are listed in Table VI. The stress-displacement plots

TABLE V Composition and physical properties of green and sintered ceramics

| Formulation | SiO ₂ Weight content (%) | Green density (g/cm ³) | Ceramic density (g/cm ³) | Theoretic density* (g/cm ³) | Theoretic mullite content (weight %) |
|-------------|-------------------------------------|------------------------------------|--------------------------------------|---|--------------------------------------|
| XMA | 3.1 | 2.52 ± 0.01 | 3.64 ± 0.01 | 3.72 | 10.15 |
| THA2 | 1.3 | 2.62 ± 0.01 | 3.12 ± 0.01 | 3.75 | 4.92 |

*Calculated according to the rule of mixtures [8] assuming that all residual silica reacts with alumina to give mullite and $\rho_{\text{alumina}} = 3.77 \text{ g/cm}^3$ (declared sintered density of SUMITOMO AES23 powder) and $\rho_{\text{mullite}} = 3.28 \text{ g/cm}^3$.

TABLE VI Mechanical properties of sintered ceramics

| | Modulus E(GPa) | Theoretical Modulus*(GPa) | σ_r (Mpa) |
|------|----------------|---------------------------|------------------|
| TMA2 | 53 | 361 | 76.4 |
| THA2 | 96 | 377 | 143 |
| XMA | 163 | 375 | 170 |

*Calculated according to Halpin-Tsai equation [8] using $\xi = 2$ for spherical like particles, and assuming that all residual silica reacts with alumina to give mullite. The modulus of alumina has been assumed to be 380 GPa. The modulus of mullite has been assumed to be 69 GPa.

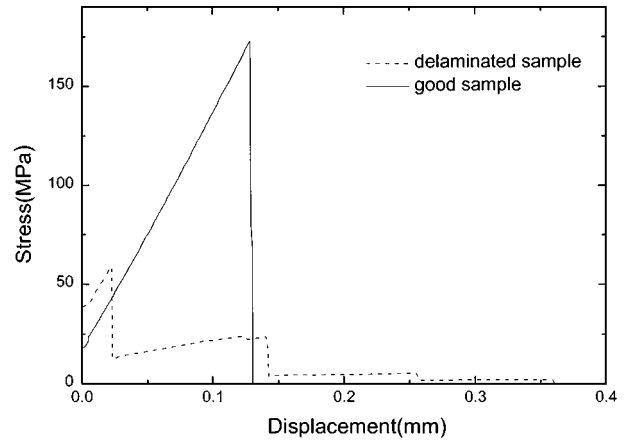


Figure 9 Stress-displacement curve obtained from a three point bending test performed on a ceramic sample built from XMA suspension.

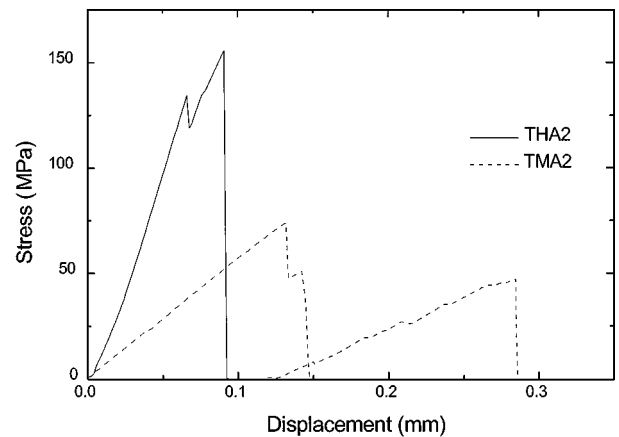


Figure 10 Stress-displacement curve obtained in three point bending tests performed on ceramic samples built from THA2 and TMA2 suspensions.

are shown in Figs 9 and 10. As shown in Table VI, the flexural moduli, compared with those calculated using Halpin-Tsai equation [8] with $\xi = 2$ for spherical like particles in the assumption that all residual silica reacts with alumina to give mullite, are much lower than theoretical values. Ceramic parts obtained

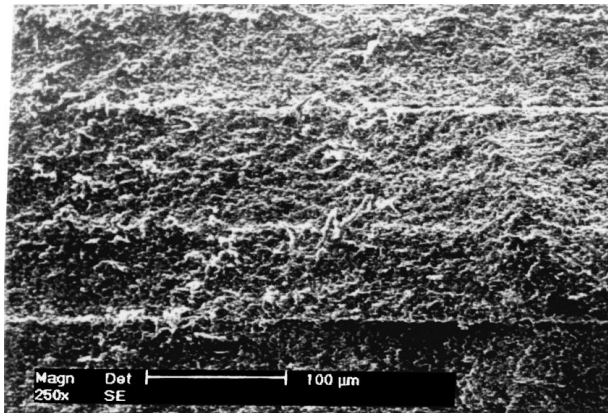


Figure 11 Image from SEM analysis of a ceramic sample obtained from XMA suspension, which show delamination at the interface between adjacent layers.

from TMA2 and THA2 undergo delamination during bending test, as indicated by the characteristic saw-teeth graphics. Only one of the ceramic specimens obtained from XMA, which is the suspension richer in alumina and residual silica (Table I), did not show any delamination. The interface between different layers built in the stereolithographic equipment appears as the weakest part due to a local higher concentration of voids where the crack can be generated and propagated during mechanical testing. The thermal treatments also may be responsible of the development of internal stresses. In fact, the only specimen which is not delaminated after sintering is obtained with the highest content of alumina and mullite and hence is subjected to lower shrinkage.

An image obtained from SEM analysis on a fractured section of a XMA sample, showing layer separation, is reported in Fig. 11. It can be noted that the interface between adjacent layers is poorer of alumina with respect to the average content. These inhomogeneities may occur as a consequence of alumina segregation to the bottom of each suspension monolayer during the STL process determining the upper zone of the monolayer to be poorer in alumina with an associated more critical shrinkage and less efficient sintering.

The delaminations may be also caused by the so called “skin effect” [9] reported for particulate reinforced composites. In this case, a reduced alumina content at the surface is attributed to the shear stresses acting on the suspension during deposition. This is a further indication of the fact that the alumina content in STL suspension is a key factor in order to obtain ceramic parts possessing good physical and mechanical properties.

4. Conclusions

– Ceramic objects, from photoactivated ceramic suspensions, are obtained using a stereolithographic apparatus. A good compromise between the reactive prop-

erties of the suspensions and their viscosity is the key factor for the development of preceramic suspensions;

– The thermal treatment led to a dense ceramic, with a superficial area approaching zero;

– The use of silicone based resins allowed improved density and better sintering especially with more than 50% of alumina particles;

– The volumetric content of alumina is a crucial matter of the process, since the parts obtained from suspensions richer in alumina show better properties in terms of density, shrinkage, mechanical properties;

– Mechanical properties ranging from 25% to 50% of those reported in literature for bulk and dense alumina are obtained;

– Future investigations will be devoted to optimise the process and the mechanical performances, improving the rheological properties of suspensions and increasing the alumina content. Furthermore a deeper analysis of the STL process parameters (linewidth compensation factor, shrinkage compensation factors in plane and cure depth) relating the final dimensions of the sintered parts to the CAD model is needed.

Acknowledgements

The research was carried out in the frame of the contract ENEA/PASTIS-CNRS within project ENEA-MURST (project 4335/04). The authors would like to thank Dr. R. Terzi and Mrs M. Schioppa, for TMA characterisations, Mrs D. Carbone for viscosity measurements, Mr. S. Mazzarelli for technical support in suspension preparation and CETMA consortium for the use of the experimental STL apparatus. Finally, professor Luigi Nicolais is gratefully acknowledged for the useful discussions.

References

1. P. F. JACOBS, “Rapid Prototyping and Manufacturing” (SME, Dearborn, USA, 1992).
2. C. I. ALWOOD, M. C. MAGUIRE, B. T. PARDO and A. A. BRYCE, *SAMPE J.* **32** (1) (1996) 55.
3. M. BURNS, “Automated Fabrication Improving Productivity in Manufacturing” (Prentice Hall, 1993).
4. M. J. EDIRISINGHE, *Mat. World* **5** (1997) 138.
5. M. AGARWALA, D. BOURELL, J. BEAMAN, H. MARCUS and J. BARLOW, *Rapid Prototyping J.* **1** (1995) 26.
6. G. A. BRADY and J. W. HALLORAN, *J. Mater. Sci.* **33** (1998) 4551.
7. CIBA-GEIGY, Technical data sheet.
8. B. D. AGARWAL and L. J. BROUTMAN, “Analysis and Performance of Fiber Composites” (John Wiley & Sons, Inc. USA).
9. L. E. NIELSEN and R. F. LANDEL, “Mechanical Properties of Polymers and Composites” (Marcel Dekker, USA).

Received 3 November 1999

and accepted 17 May 2000